UNIVERSITAT POLITÈCNICA DE VALÈNCIA

ESCOLA POLITECNICA SUPERIOR DE GANDIA

MASTER EN EVALUACIÓN Y SEGUIMIENTO AMBIENTAL DE ECOSISTEMAS MARINOS Y COSTEROS

UNIVERSITAT POLITÈCNICA DE VALÈNCIA

ESCOLA POLITÈCNICA SUPERIOR DE GANDIA

"Tidal dynamics effect on the connectivity patterns of the blackspot seabream (*Pagellus bogaraveo)* in the Alboran Sea"

TRABAJO FINAL DE MÁSTER

Autor/a:

IRENE NADAL ARIZO

Tutor/a:

DR. VICTOR SÁNCHEZ MORCILLO
DR. JESÚS GARCIA LAFUENTE
DR. SIMONE SAMMARTINO

GANDIA, 2019

AGRADECIMIENTOS

En primer lugar, quería agradecer al Grupo de Oceanografía Física de la Universidad de Málaga por otorgarme la oportunidad de realizar las prácticas con ellos. En especial, a mis tutores de centro, Jesús García Lafuente y Simone Sammartino, quienes me han enseñado, guiado y supervisado durante el desarrollo completo del trabajo con mucha comprensión. A pesar de la dificultad que para mí suponía, me habéis hecho disfrutar de este trabajo como nunca y habéis despertado en mi un deseo por seguir investigando. También a Cristina Naranjo y Jose Carlos Sánchez, por haber sido un apoyo e inspiración constante y haber hecho mi estancia en el grupo mucho más bonita. ¡¡Os admiro mucho a todos‼ Gracias de corazón.

A mi tutor y coordinador Víctor Sánchez Morcillo, gracias por haberme inspirado y motivado a la realización de este trabajo con el que he disfrutado tanto.

A Andy, que buenos recuerdos de Málaga me traes. Muchas gracias por haberme ayudado con la búsqueda de becas y haberme animado con esos paseos a la hora de la merienda por la UMA.

A todos mis compañeros del máster, pero en especial a Judith y Carlos, que más que compañeros son amigos. Gracias por haberme escuchado, acompañado y aconsejado en todo momento.

Una vez más, a Adri. Gracias por tu infinita paciencia, por tu ayuda constante y sobre todo, por acompañarme en un camino que acaba de empezar. Sigues demostrándome que con esfuerzo todo se consigue y que rendirse no es una opción. Ojalá puedas seguir recordándomelo siempre.

Por último, gracias a mis padres, por apoyarme y ayudarme a seguir mi vocación.

Index

Abstract

The blackspot seabream [*Pagellus bogaraveo* (Brünnich, 1768) is a highly appreciated species both for its economic and gastronomic value in the Strait of Gibraltar. Nevertheless, for the same reason, is also one of the more over-exploited species, which has caused a significant decrease in catches over the years. Experts in fishery ecology agree that for optimizing the fisheries as well as curbing the over-exploitation is necessary to study population dynamics and connectivity. Thus, with the aim of better understanding the population dynamics of this species, as well as determining its general dispersion patterns in the Alboran Sea, the hydrodynamic connectivity of the blackspot seabreams in Early Life Stage (eggs and larvae) has been investigated by means of a numerical model, using a lagrangian approach. The releases of the passive particles (simulating ELS pathways) were implemented under different tide conditions (according to the tidal phase and strength), depths and area of origin. It was determined that the fortnightly modulation (spring tide-neap tide) is the main factor driving the horizontal dispersion of eggs and larvae.

Keywords: blackspot seabream, early life stage, lagrangian algorithm, tidal dynamics, Alboran Sea

Resumen

El voraz [*Pagellus bogaraveo* (Brünnich, 1768)] es una especie altamente apreciada tanto por su valor económico como gastronómico en el Estrecho de Gibraltar. No obstante, por esta misma razón, es también una de las especies más sobre-explotadas de la zona, lo que ha provocado que las capturas hayan descendido significativamente a lo largo de los años. Dentro del ámbito científico, existe un consenso que considera que para optimizar las pesquerías a la vez que dejar de sobre explotar este recurso, es necesario hacer estudios de dinámica poblacional y conectividad. Por tanto, con el objetivo de conocer mejor la dinámica poblacional de la especie, así como sus mecanismos de dispersión en el Mar de Alborán, se analizó su conectividad hidrodinámica a partir de un modelo numérico, utilizando voraces en estadios de vida temprana (huevos y larvas) como partículas virtuales lagrangianas (advectadas por la dinámica mareal). Los lanzamientos de las partículas se realizaron bajo diferentes condiciones de marea (en función de la fase y el ciclo mareal), profundidad y zona de suelta. Se determinó que la modulación marea viva-marea muerta es, en este caso, el factor predominante para la dispersión horizontal de los huevos y larvas de esta especie.

Palabras clave: voraz, estadios de vida temprana, algoritmo lagrangiano, dinámica mareal, mar de Alborán.

I. Introduction

Geomorphologically, the Mediterranean Sea is separated from the Atlantic Ocean by the Strait of Gibraltar (SoG), a connection of 14 km width and 300 m depth approximately in its shallowest sill (Rodríguez, 1982) which allows, in turn, the existence of a transition sea situated in the most western region of the Mediterranean Sea, known as the Alboran Sea. This particular region is limited, on its western edge, by the own Strait, and on its eastern edge, by the imaginary limit Cape Gata (Almería) - Cape Fegalo (Oran).

The snappish separation between the Atlantic Ocean and the Mediterranean Sea causes that, the North Atlantic Central Water (NACW), which is considerably fresher and warmer than the outflow water mass, is forced to emerge as a surface layer narrowing eastwards throughout the SoG. On the other hand, a mix of the Western Mediterranean Deep Water (WMDW), the Levantine Intermediate Water (LIW) and other less abundant and intermittent water masses as the Tyrrhenian Dense Water (TDW) and the Winter Intermediate Water (WIW) (Toucanne *et al.,* 2014), all named as Mediterranean Outflow Water (MOW), which are saltier, colder and, thus, denser than the NACW, tend to leave the Alboran basin through the bottom and spread to deeper layers into the Atlantic Ocean. The separation between NACW and MOW is not abrupt, in fact, it forms a transition layer (interface) of intermediate characteristics , whose thickness and depth vary notably both spatially, throughout the whole Strait, and temporally, both at tidal and subtidal time scale (García Lafuente *et al.,* 2013).

As a consequence of the marked gradient pressure in the zone, the Earth's rotation effect and the geomorphology variation, there is a substantial difference in the tidal range between the two sides of the Strait. In the Gulf of Cadiz (western edge of the SoG) the tidal range can exceed 3m while in the Alboran Sea, sea level variations rarely overpass 1m (Candela *et al.,* 1990). As a result of that difference an area of intense tidal currents is originated, moving huge volumes of water backward and forward the SoG, creating a pulsating dynamic.

a. General circulation of the Alboran Sea

The general circulation pattern in the Alboran Sea is basically characterized by a strong quasi-permanent surface current (Atlantic Jet, AJ hereinafter) that intrudes on the basin from the SoG. The AJ flows with an estimated speed of 1-2 $m \cdot s^{-1}$ (García Lafuente *et al.,* 2000) and, as a consequence of the Coriolis force, surrounds and feeds two high pressure anticyclonic (clockwise) gyres: the Western Alboran Gyre (WAG)

and the Eastern Alboran Gyre (EAG) (JC Sánchez Garrido *et al.,* 2013). The WAG, generally larger and more stable than the EAG, is located at the western half of the basin (1200 m depth) between the SoG and approximately 3° W longitude, whilst the EAG, which is usually smaller and more intermittent, is situated over the eastern basin (1800 m depth) between 3° W and 1.5° W longitude (Renault *et al.*, 2012; Lafuente *et al.,* 1998). Between the WAG and the EAG, at 3° W approximately, the low pressure (anticlockwise) Central Cyclonic Gyre (CCG) can be found, which is considerably smaller and less energetic than the previous two (Renault *et al.,* 2012). Moreover, other analyses show the existence of several cyclonic instabilities or eddies throughout the northern boundary of the WAG, which can induce upwelling in a high productivity area (Sarhan *et al.,* 2000). The general circulation pattern is shown in Figure 1.

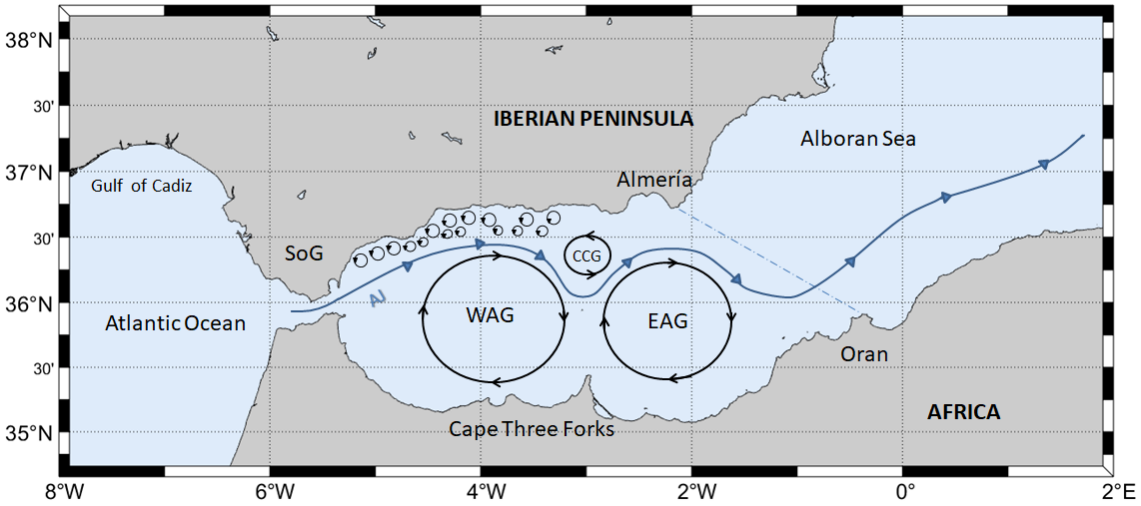

Figure 1. General circulation pattern of the Alboran Sea. Sketch adapted from Sánchez-Garrido *et al.*, 2013. AJ, WAG, EAG CCG and small eddies throughout the northern boundary of the WAG are shown as solid thick lines and arrows. The imaginary limit Cape Gata (Almería) - Cape Fegalo (Oran) is displayed as a dashed line.

According to some authors (Lafuente *et al.,* 2002; Vargas-Yáñez *et al.,* 2002), during the winter period, the AJ, subjected to higher variability, can weaken and deflect toward the African coast (because of the Coriolis force). When it occurs the two gyres tend to destabilize, lose intensity and even vanish.

b. Oligotrophy and productivity of the basin

Many studies based on the analysis ocean color satellite images, water column profiles and other methods, coincide on the idea that the Mediterranean is an oligotrophic sea, which means, low primary production as a result of a low nutrient content. One of the most consensual reasons is based on the fact that although the NACW that enters from the SoG is limited to a superficial layer and is considerably

poorer in nutrients (nitrates and phosphates principally) than the underlying MOW outgoing (Rodríguez, 1982), which nutrient content is generally higher due to organic matter remineralization, it is still more productive than the Mediterranean waters located at the same level.

The low nutrient concentration is clearly observed in both anticyclonic gyres (WAG+EAG) where, as a consequence of the Ekman dynamics, it produces a convergence (*downwelling*) of the surface waters to deeper layers. This process causes the surface layer to turn warmer and more oligotrophic as the waters sink.

On the other hand, in cyclonic gyres, surface waters are replaced by cold and nutrient-rich waters from deeper layers. For this reason, the northern boundary of the Alboran Sea (where cyclonic eddies are more frequent) is characterized by a high biologic productivity area stimulated by the existence of divergence (*upwelling*). As the previous case, this process becomes more evident in summer, when thermal gradient contrast is stronger (Sarhan *et al.*, 2000; José C Sánchez Garrido, Naranjo, Macías, García-Lafuente, & Oguz, 2015).

There are several reasons why cyclonic gyres and, therefore, upwelling phenomena, occur in these particular areas of the Alboran Sea. According to authors like Sarhan *et al.,* 2000, the most significant of them is that they are induced by westerlies winds, which replace surface waters offshore causing them to sink. Other authors (José C Sánchez Garrido *et al.* (2015) or Navarro *et al.* 2011)) refer to the high concentrations of superficial chlorophyll pigments inflowing with the AJ. This reason can be evidenced by *in situ* observational data and ocean color satellite images, that provide information of phytoplankton biomass, primary production or vertical fluxes, among many other aspects (Reul *et al.,* 2005). Other authors argue that the process can be induced by occasional unsteadiness of the AJ previously mentioned (Vélez Belchí *et al.,* 2005, J C Sánchez Garrido *et al.,* 2013). Moreover, there are other mechanisms that, despite being unusual and not entirely evidenced, can provide upwelling conditions. One of them is due to eventual unsteadiness of the cold Mediterranean water, which frictions with the Atlantic water and produces vertical transports because of the geostrophic balance effect (Sarhan *et al.,* 2000). Finally, complex bottom topography, submarine canyons or other irregularities have been noticed by other author as probable causes of deep waters and upper waters exchange, originating a divergence phenomenon (Rodríguez, 1982).

c. Fishes connectivity patterns

The favorable conditions of the Alboran Sea upwelling areas allow phytoplankton fast growth and, consequently, high primary production. This increases zooplankton and ichthyoplankton to a large degree, thus being a more favorable area for spawning fishes season, which generally becomes more intense during spring and autumn, coinciding with higher productivity (Sarhan *et al.,* 2000). In this framework, the general circulation patterns and their variability in speed and location as a consequence of the environmental dynamics, as wind, tidal forces, surface waves, advection, diffusion and turbulence, among others, are believed to play a key role in the dispersion of propagules, maximizing the distribution of the species over the maximum geographical range and, thus, connecting marine species populations. This interaction between fish propagules and the dynamic conditions of the marine environment is termed by the concept of dynamic connectivity. In other words, dynamic connectivity can be defined as the linkages and connections of eggs and larvae single species from a dynamic point of view in different spatial and temporal scales (Cowen and Sponaugle, 2009).

The knowledge of dynamic connectivity of a specific species has many utilities in scientific researches towards their better management. In fact, there is a common consensus among the scientific community that affirms that, before doing any management study, it is necessary to understand the connectivity of the species according to the circulation and oceanographic variability (Cowen and Sponaugle, 2009; Urban and Pratson, 2008) . The main applications of the connectivity studies are aimed to improving the knowledge of the fish population dynamics in order to optimize the fisheries management, especially those that have over-exploited target fishes (Sammartino *et al.*, 2018; Fuller *et al.*, 2017; Sahyoun *et al.*, 2017; Feist *et al.*, 2010; Botsford *et al.*, 2009). In this framework, several researchers have reported that many fish populations in the Mediterranean Sea, mainly around western regions are subjected to an excessive exploitation over the years(Muñoz et al., 2015; UNEP, 2014; García et al., 2012; Gil Herrera, 2006; Reul et al., 2005).

Thus, in order to maintain the sustainability of the most important marine resources and fisheries in the central and western Mediterranean Sea, the Fisheries and Aquaculture Department Food and Agriculture Organization (FAO) decided to carry out the second phase of the *Coordination to Support Fisheries Management in the Western and Central Mediterranean program*, known as CopeMed II (GCP/INT/317/EC Year 09), currently in process, which was built on the achievements of the first phase (CopeMed I, 1996-2005). As a secondary aim of this project, the sub-

program *Transboundary stock structure of sardine, black spot seabream and hake in the Alboran Sea and adjacent waters,* known with the acronym of TransBoran, was defined with the purpose of identifying the connectivity stocks of three interesting target species in the SoG and the Alboran Sea: the hake [*Merluccius merluccius* (Linnaeus, 1758)], the sardine [*Sardina pilchardus* (Walbaum, 1792)] and the blackspot seabream [*Pagellus bogaraveo* (Brünnich, 1768)].

One of the main tasks of the Transboran program, which are already being done by the Physical Oceanography Group of the University of Malaga (GOFIMA), is the study the hydrodynamic connectivity, i.e., the description of the hydrodynamic effect in the connectivity patterns, using numerical experiments by supercomputing resources.

Within the framework of this collaboration task, focused on improving the conservation of the mentioned species, the study of the blackspot seabream connectivity is particularly important, given the commercial value of that species and the advanced status of its overexploitation (Gil Herrera, 2006). The present work is framed in this collaboration context.

II. The Blackspot seabream (*Pagellus bogaraveo*)

The blackspot seabream is a teleost demersal fish belonging to the Sparidae family (Figure 2). It inhabits above several types of bottoms (rocky, sandy or muddy) and has a wide distribution across the Eastern Atlantic Ocean and the Mediterranean Sea, reaching up to 700m and 400m depth respectively (Gil Herrera, 2006).

Figure 2. The blackspot seabream [Pagellus bogaraveo (Brünnich, 1768)] Draw of Carmen B. de los Santos adapted from (Gil Herrera, 2006).

Spawning stage of the adult blackspot seabream occurs in the SoG shallow zones between October and April, being the most intense period from December to March (Gil Herrera, 2006). According to Machperson and Raventos (2006) and Gil Herrera (2006) among many other authors, after this process, fertilized eggs go through a difficult phase of their life cycle known as Early Life Stage (ELS) which lasts, approximately, between 40 and 60 days (Pelagic Larval Duration, PLD). Then, surviving specimens spend the first year of their life in coastal zones, such as bays,

breakwaters and even inside the ports until reaching a size of around 15 cm. Following that period, they migrate to deeper adjacent zones in the SoG. It is a protandric hermaphrodite; which means that, sometimes, once males reach sexual maturity (25 cm) and completely develop as a functional male, their male gonad degenerates and, subsequently, a female gonad develops at the same time reaching sexual maturity as a functional female (36 cm). Finally, blackspot seabream ascends to the shallower layer, to start the spawning stage again, completing life cycle.

Blackspot seabream landings at the zone (Figure 3) were 854 t in 1994, reaching the highest quantity registered to that date (ICES, 2018) but, due to a marked increase on fishing pressure, captures decreased sharply to 520 t in 1998, with the most notable drop in 1995 (625 t) (Sammartino *et al.,* 2018; Gil Herrera, 2006). As a consequence of it, the Ministry of Agriculture, Fisheries and Food (MAPAMA) of the Spanish Government, decided to impose a fishery regulation, adding a specific plan for it called *voracera* (06/17/1998 order regulation published in BOE nº157, 07/02/1998), where art technical characteristics, minimal sizes and other rules are clarified. In the following years, catches continued falling reaching a minimum of 248 t in 2002 (Gil Herrera, 2006). Landings started increasing reaching 578 t in 2009; nevertheless, after that, an abrupt decrease occurred again with a minimal historic value of 60 t in 2012. Currently, landings are staying at similar values (ICES, 2018).

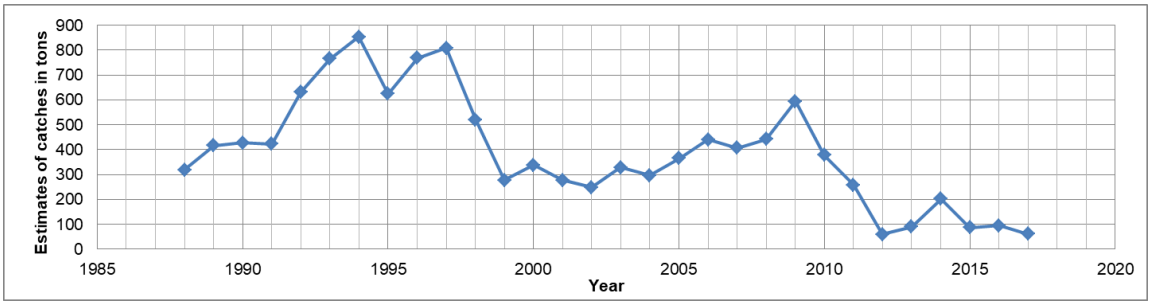

Figure 3. Estimates of the blackspot seabream catches in tons at the Subarea 9 over the years (ICES, 2018; Gil Herrera, 2006)

III. Justification and objectives

In accordance with the explained above, it becomes evident that the study of hydrodynamic connectivity is essential for a comprehensive understanding of the fish populations dynamics and, thus, for improve the species management from an economically point of view. To estimate the dispersal pathways and connectivity patterns is necessary to know the hydrodynamic features of the specific zone, and the most appropriate tool in these cases is the numerical models. In fact, the connectivity studies based on the output of Lagrangian models are of paramount importance in support to fisheries management and optimization. Specifically, understanding

blackspot seabream connectivity and its general dispersal patterns according to the Alboran Sea and the SoG tidal dynamics in different temporal and spatial scales, could allow a better management of *voracera's* fleets, avoiding a continuous over-exploiting of them.

Thus, taking all the explained into account, the general objective of this work is to analyze the blackspot seabream connectivity from a hydrodynamic numerical model using early life stage (ELS) blackspot seabream virtual particles as passive tracers advected by dynamical tides. ELS blackspot seabreams were used because it is considered that, once they overcome that phase, they have enough swimming capacity for not being transported passively by the current.

To achieve this general objective, several sensitivity analyses in function of its special and temporal variability were necessary to do. In order to determine the spatial sensitivity according to the release zone, three release boxes were defined in the SoG area, due to is the blackspot seabream most spawning active zone. Moreover, the depth level had to been taken into account for a complete comprehension of the interaction between different vertical levels. Thus, five release depths were included in the experiments. On the other hand, with the aim to determine the temporal sensitivity to the model results, eight tide combinations according to the tide phase and strength. Finally, four replicas were established to compare the results between different time series.

IV. The numerical model

The model used in this paper to carry out numerical simulations is the Massachusetts Institute of Technology general circulation model [MITgcm (Marshall *et al.*, 1997)], widely employed to describe successfully the complex dynamics of the study region. The code solves the incompressible simplification Boussinesq form of the Reynolds-averaged Navier-Stokes equations (1) with a hydrostatic formulation. It is written in FORTRAN, a programming language commonly used in computational fluid dynamic field, and is operated on LINUX computing operating system.

$$\frac{\partial u}{\partial t} + u\frac{\partial u}{\partial x} + v\frac{\partial u}{\partial y} + w\frac{\partial u}{\partial z} = -\frac{1}{\rho}\frac{\partial p}{\partial x} + 2\Omega v \sin\varphi + F_x$$

$$\frac{\partial v}{\partial t} + u\frac{\partial v}{\partial x} + v\frac{\partial v}{\partial y} + w\frac{\partial v}{\partial z} = -\frac{1}{\rho}\frac{\partial p}{\partial y} - 2\Omega u \sin\varphi + F_y \quad (1)$$

$$\frac{\partial w}{\partial t} + u\frac{\partial w}{\partial x} + v\frac{\partial w}{\partial y} + w\frac{\partial w}{\partial z} = -\frac{1}{\rho}\frac{\partial p}{\partial z} + 2\Omega u \cos\varphi - g + F_z$$

The model domain spans from the Gulf of Cadiz (9.37° W), through the SoG to the Alboran Sea eastern edge (1.59° E), throughout a curvilinear horizontal grid, with variable resolution, maximum in the Strait region. The vertical discretization is uneven, with maximum resolution at surface (Figure 4).

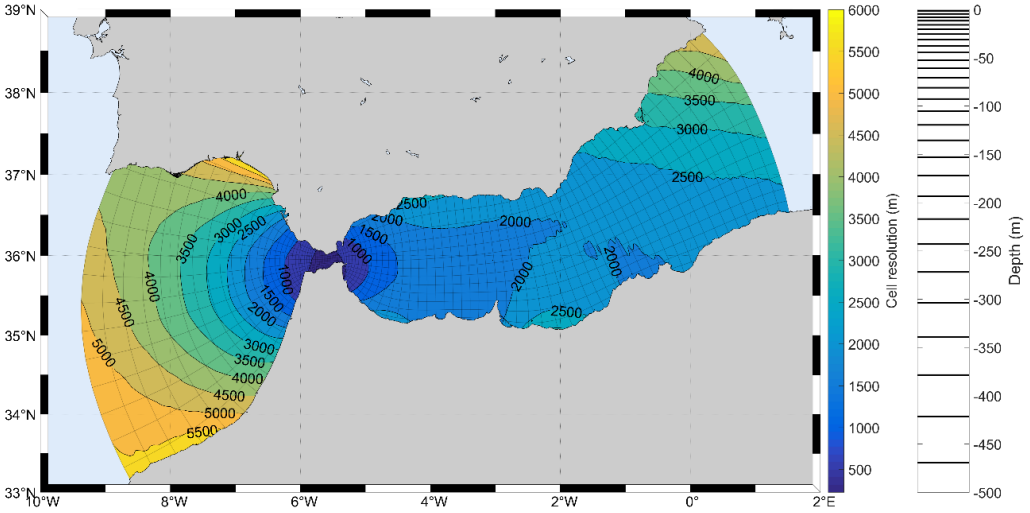

Figure 4. Model domain, with horizontal (one every 7 cells has been displayed for clearness) and vertical grid (up to 500m depth).

The model was forced with different sources at its open boundaries. The IBI (Iberian Biscay Irish) Ocean Reanalysis system (Sotillo *et al.,* 2015) provided the horizontal current, temperature and salinity baroclinic fields to prescribe oceanographic conditions at the lateral open boundaries. The storm surge NIVMAR model (García Lafuente *et al.,* 2002; Álvarez Fanjul *et al.,* 2001) allowed the incorporation of the barotropic velocity field to the lateral boundaries, with the aim to apply the atmospheric pressure effect on the water exchange through the SoG. Finally, air temperature and humidity, precipitation and heat fluxes were prescribed at the surface open boundary by the atmospheric model HIRLAM, by the Spanish Meteorology Agency.

The general configuration of the model, its advection and vertical mixing scheme is described in detail in Sammartino *et al.,* (2014). The model run in the PICASSO cluster of the Supercomputing and Bioinnovation Center of the University of Málaga, and simulated a total of 6 month hindcast, recording the zonal and meridional components of the horizontal velocity every 30 minutes.

Due that the aim of the model is to reproduce the blackspot seabream dynamics in the ELS phase, the simulated hindcast corresponds with the most active spawning stage that, as previously mentioned, covers the first trimester of the year. In particular the period November 2004 April 2005 was simulated, with a spin-up time of one month, such that the recorded fields span from December 2004 to April 2005.

Figure 5 shows the general circulation as provided by the forcing model CMEMS-IBI. WAG and EAG are clearly visible in the maps by large (red) positive anomalies and anticyclonic/clockwise circulation, while, CCG and small eddies throughout the Alboran Sea northern boundary are identified by blue colors and arrows in cyclonic/anticlockwise direction.

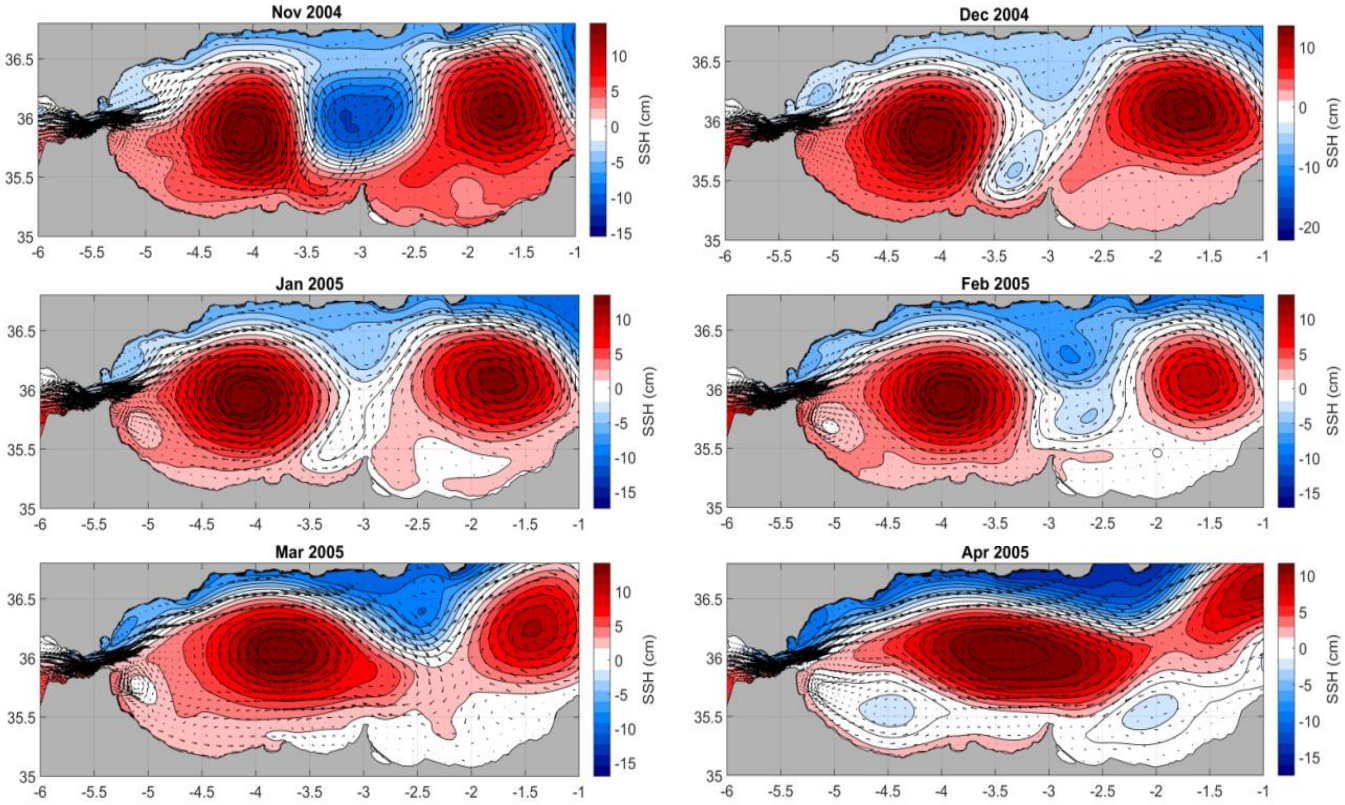

Figure 5. Sea Surface Height (SSH) for the simulated period 11/2004 – 04/2005 Blue and red colors display the negative and positive anomaly, respectively. Mean surface velocity field is displayed by arrows, which indicate the flow direction.

V. Lagrangian particle tracking algorithm

To assess the dynamic interaction of ELS blackspot seabream with marine environment, a lagrangian particle tracking (LPT) algorithm was used, as a virtual passive observational method. Lagrangian simulations, unlike eulerian, are an effective way to the study the general pattern of connectivity between different sub-areas as a result of observing the advection of eggs and larvae (that, numerically, are considered as passive particles) under the effect of the current (LaCasce, 2008). For this particular case, LPT was based on the Runge-Kutta 4 th order method.

Lagrangian particles were simulated under different spatial and temporal combination of conditions to investigate how different tides affect them. First, to see the particles behaviour according to the release area, three starting areas were defined within the SoG: Tanger, TangerMED and Tarifa. On the other hand, ten possible

destination areas were defined: Cadiz, Estepona, Malaga, Roquetas, Carboneras, Oran, Melilla, Alucemas, Tetuan and Arcila (Figure 6)

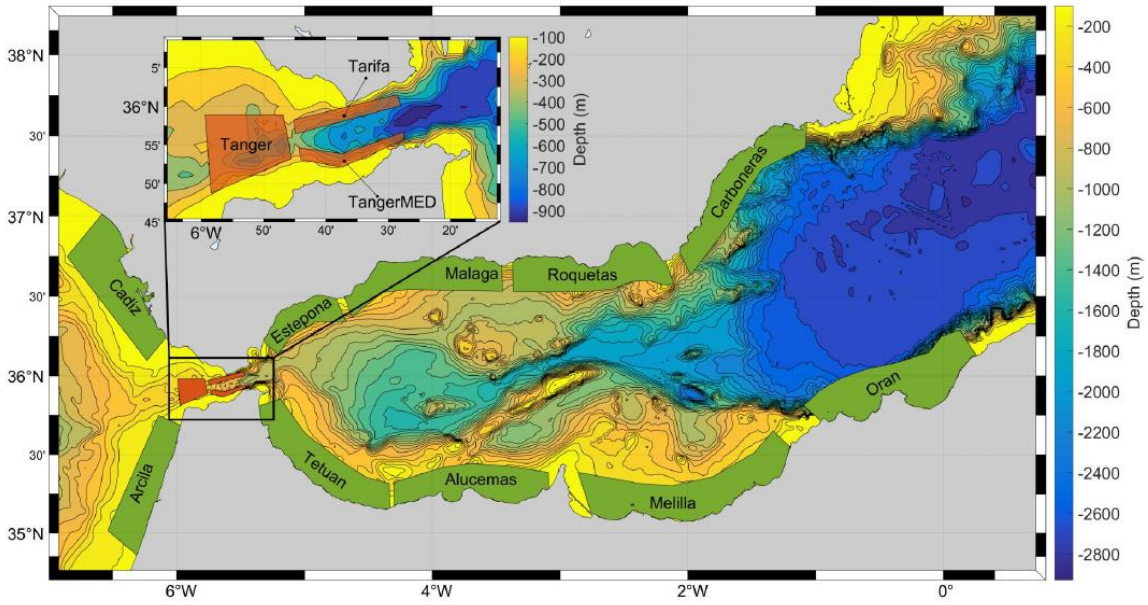

Figure 6. Three release areas (Tarifa, Tanger and TangerMED) and ten adjacent connectivity boxes (Cadiz, Estepona, Malaga, Roquetas, Carboneras, Oran, Melilla, Alucemas, Tetuan and Arcila).

Secondly, to see the particles behaviour at several vertical levels, five release depths were considered, at 1m, 12m, 25m, 52m and 81m.

Third, with the aim of estimating the effect of tides on the ELS dispersal patterns, an array of LPT simulations have been started under a set of eight tide combinations of the different conditions depending on the tidal phase [(H) High, (L) Low, (F) Flood, (E) Ebb tide] and the tide strength [(S) Spring, (N) Neap tide] (Figure 7). Finally, with the aim of obtaining a more robust estimation of the metrics used, a total of four replicas for each of the aforementioned condition, were implemented throughout the first two months of 2005.

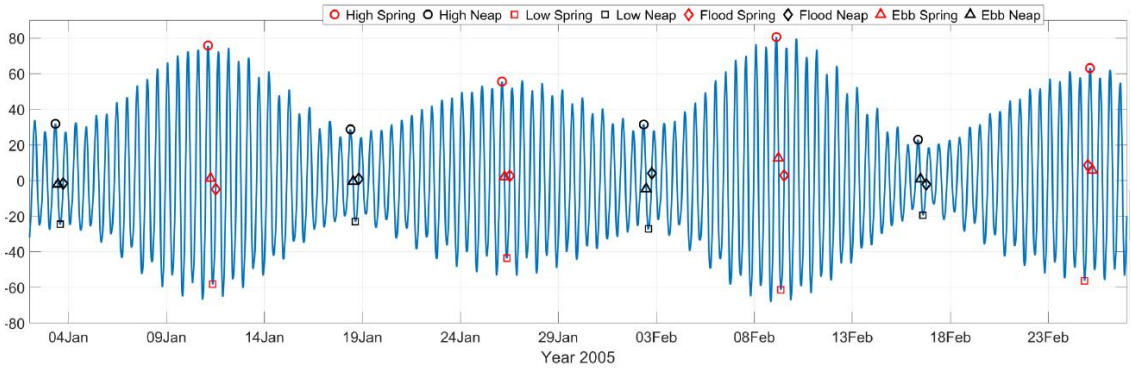

Figure 7. Starting times of the Lagrangian Particle Tracking (LPT) according to the different tide combinations and replicas.

Each single LPT simulation lasted for 60 days. In order to optimize the computational cost of the algorithm, it has been parallelized, involving a total of 48 CPUs. The initial particle position was randomly assigned within the limits of the release box, with a maximum total amount of 2400 particles.

As each individual run was done by 48 CPUs at the same time the resultant output would be 48 files per run, then, the files had to be grouped in a single logical file for easier interpretation and working efficience.

Simulations results in (4 tide phase x 2 tide strength x 4 replicas x 5 depths) 160 runs per release areas, according a total of 480 runs. Because of the random seed of the initial particles positions and the different geometry of the release areas, the number of particles varied for each run, with averages values of:

- 780.7 particles in Tarifa release area (Figure 8a).
- 1731.2 particles in Tanger release area (Figure 8b).
- 765.4 particles in TangerMED release area (Figure 8c).

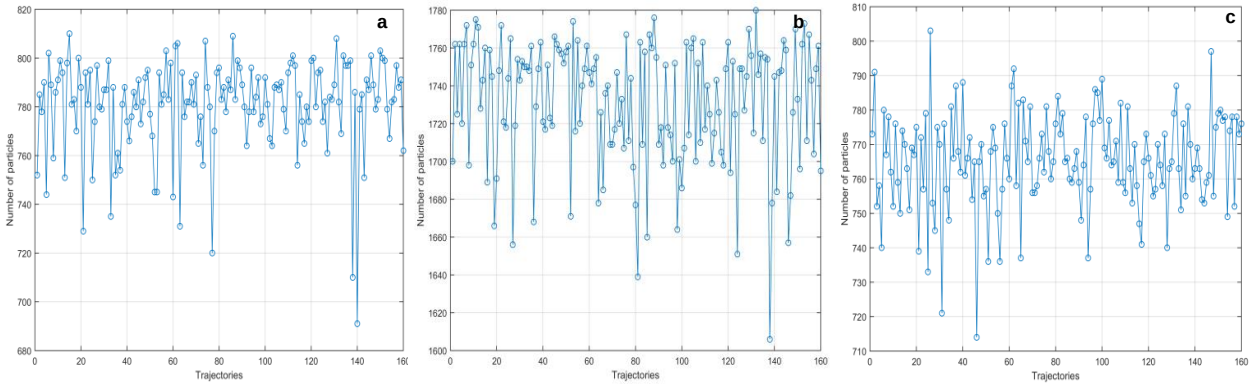

Figure 8. Particles released in Tarifa (a), Tanger (b) and TangerMED (c). See also Figure 6.

VI. Results and discussion

Because of the high energetic dynamics and variability of the study area, and the strong current acting in there, a fixed time metric (percentage of particles released in box *a* and found in box *b*, at specific time *t*) was not convenient to use. Hence the maximum percentages of particles observed in all the connectivity boxes, and the corresponding times have been considered. Table 1 shows the averaged ELS percentages (over the four replicas) as well as the coefficient of variation for each release area.

Table 1. Mean ELS percentages and the corresponding coefficient of variation for Tarifa, Tanger, TangerMED and Tarifa release areas.

Connectivity box		Averaged connectivity (%)		
		Tarifa	Tanger	TangerMED
Northern limit	Cadiz	0.10 ± 0.00	0.03 ± 0.00	0.00 ± 0.00
	Estepona	37.91± 0.67	9.56 ± 0.63	8.38 ± 1.40
	Malaga	45.27 ± 0.26	14.85 ± 0.49	11.25 ± 1.06
	Roquetas	16.56 ± 0.80	5.45 ± 0.56	4.56 ± 0.98
	Carboneras	6.46 ± 0.52	1.96 ± 1.10	2.06 ± 0.87
Southern limit	Arcila	0.00 ± 0.00	1.47 ± 0.52	0.01 ± 0.00
	Tetuan	8.45 ± 0.87	32.60 ± 0.42	44.91 ± 0.48
	Alucemas	8.36 ± 0.68	13.75 ± 1.04	17.33 ± 0.97
	Melilla	6.20 ± 1.14	3.42 ± 0.52	3.75 ± 1.11
	Oran	13.69 ± 0.48	6.48 ± 0.21	4.66 ± 0.51

As it can be deduced, the highest values of average connectivity for the particles released from Tarifa are found in the northern limit of the Alboran Sea, whilst the highest values for the particles released from Tanger and TangerMED areas are found in the southern limit, which suggests a zonal (west-east) predominance connectivity instead of meridional (north-south) as a consequence of the stable surface current (AJ) intruding from the SoG. Specifically, the highest percentages of Tarifa are reached at Malaga and Estepona boxes, whilst the highest percentages of Tanger and TangerMED areas are reached at Tetuan and Alucemas boxes. Although Malaga is the third box located at the northern limit, a relatively high percentage, compared to others boxes of the southern limit, can be observed for Tanger and TangerMED release areas, possibly due to particles entrance on the WAG gyre after their crossing by Tetuan and Alucemas boxes. On the other hand, the lowest percentages are registered at Cadiz and Arcila boxes for the three release areas. This supports the idea that the AJ forces the released particles to disperse predominantly eastwards, in the Mediterranean basin, while only a small percentage of particles leap toward the Atlantic Ocean.

Most of the coefficients of variation are maintained at stable values between 0 and 1%, suggesting a relative homogeneity within the model results. Only in a few specific connectivity boxes (as TangerMED-Estepona or Tarifa-Melilla) this percentage is surpassed, suggesting a higher heterogeneity and dispersion of these results. Figure 9, Figure 10 and Figure 11 shows maps of the averaged maximum particles of ELS reached at all the connectivity boxes from Tarifa, Tanger and TangerMED, respectively.

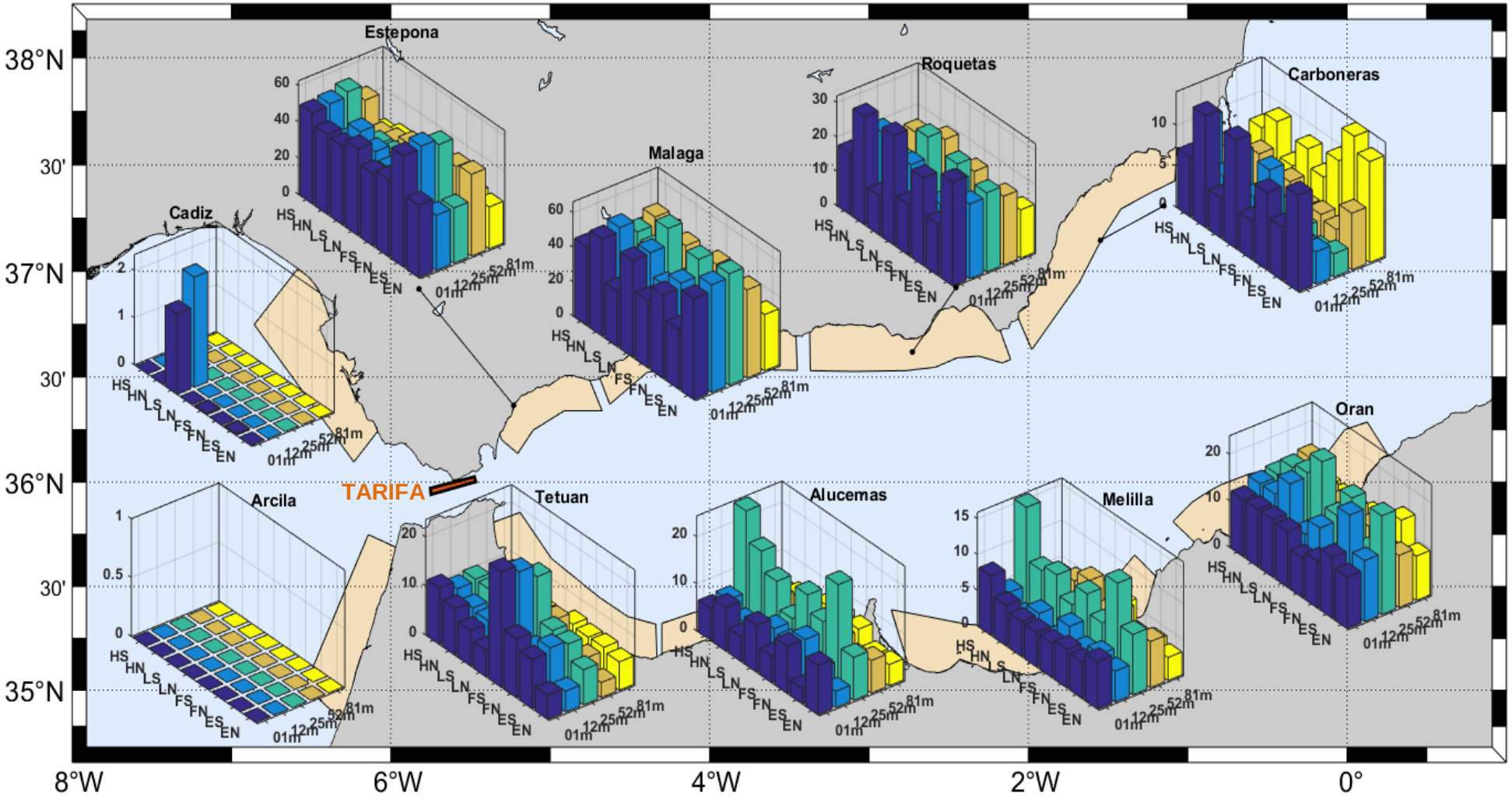

Figure 9. Map of the averaged maximum particles of ELS reached at all the connectivity boxes from the Tarifa area according to the 160 combinations and the 10 adjoining boxes.

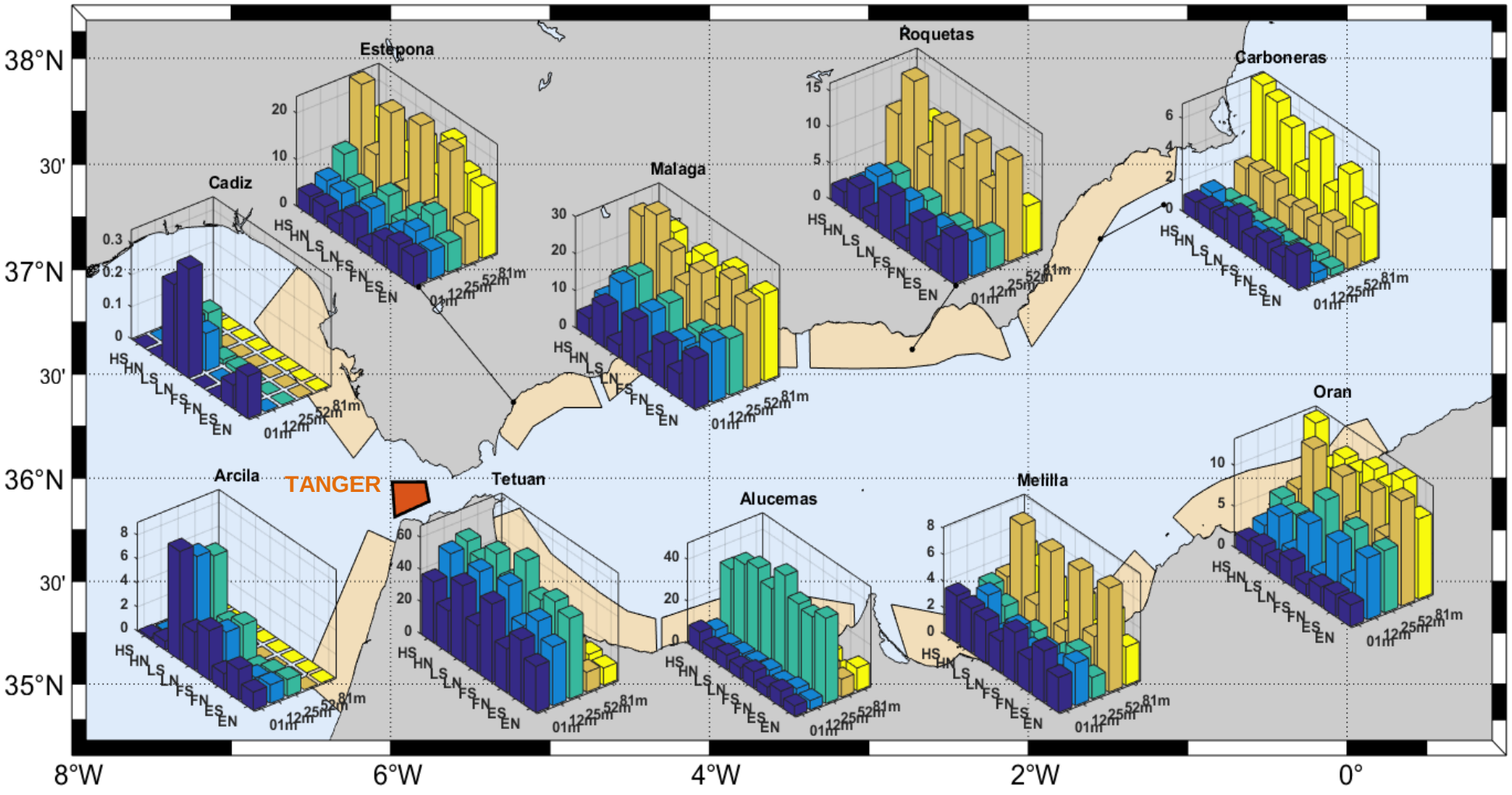

Figure 10. Map of the averaged maximum particles of ELS reached at all the connectivity boxes from the Tanger area according to the 160 combinations and the 10 adjoining boxes.

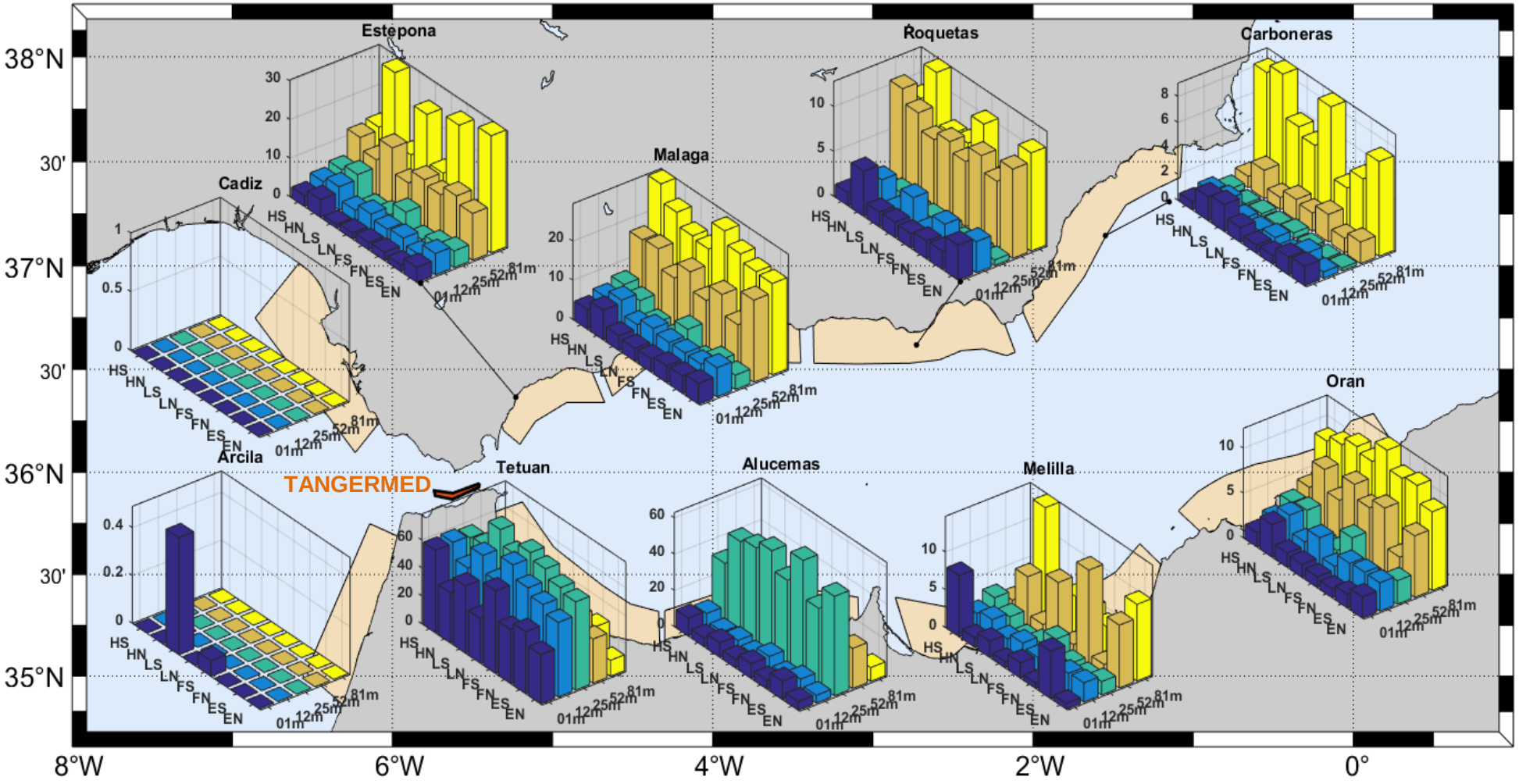

Figure 11. Map of the averaged maximum particles of ELS reached at all the connectivity boxes from the TangerMED area according to the 160 combinations and the 10 adjoining boxes.

The first map (Figure 9) shows values of ELS (%) released from Tarifa and predominantly advected along the northern margin of the Alboran Sea, being higher at Estepona (37.91%± 0.67%) and Malaga (45.27% ± 0.26%) boxes (see also Table 1).

The connectivity box Estepona (see Figure 6), for its proximity to the SoG and to the starting area, presents the earliest maximum connectivity percentages (Figure 12), and a progressive drop of values from High Tide (HS) to Low Tide, according to the general tidal modulation of the SoG exchange that prescribe the maximum (minimum) inflow and the corresponding minimum (maximum) outflow in ebb (flood) tide. The variability due to the tidal fortnightly modulation is also noticeable, especially in terms of time shift of the connectivity maxima (Figure 12), which, in turn, are not sensibly broadened.

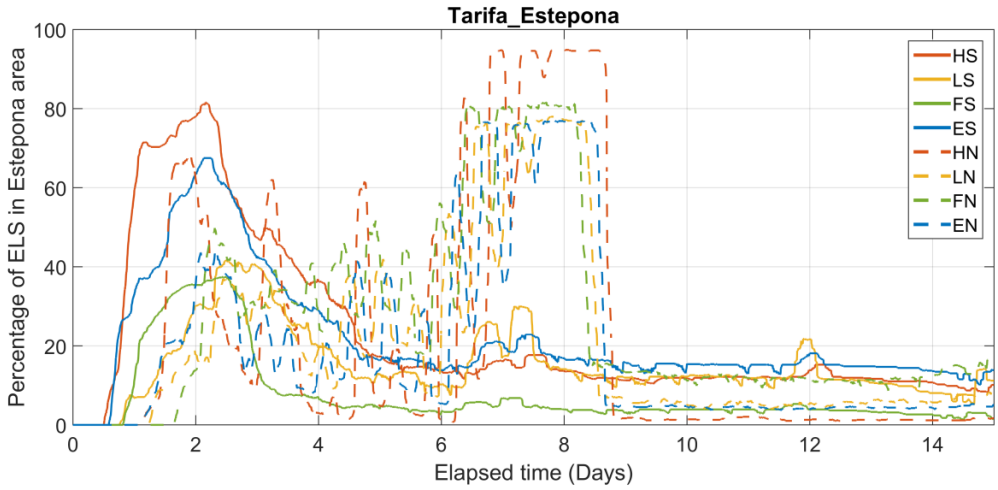

Figure 12. Percentages of ELS released at surface in Tarifa and found in Estepona box over the elapsed time under different tidal conditions. The fourth tidal phase combined with the spring cycle are displayed by solid lines, whilst the combined with the neap cycle are displayed by dashed lines.

From Malaga box to the rest of the connectivity boxes of the northern boundary, the discrepancy driven by the fortnightly modulation starts to be more evident, being more appreciable in Roquetas and Carboneras boxes under neap cycles (with differences of ≈20% and ≈10% respectively compared to the tidal combinations with spring cycles, see Figure 9 and Figure 13). This, prior to other calculations suggests a faster speed of the particles under spring cycles and, thus, a higher dispersion of the eggs and larvae in this tide condition. On the other hand, there are not big differences between the different tidal phases (high, low, ebb and flood tides) along the northern boxes, which suggest a major influence of the tidal strength for the particles released in this area.

Figure 13 provides a clear example of it. As expected, the percentage of ELS registered and the corresponding elapsed time were lower under the spring cycle (≈40% at the ≈6 day), whilst the percentage registered under neap cycles and its corresponding time, were significantly higher (≈80% at the ≈4 day), which affirmed the lower dispersion and velocity of the eggs and larvae under this cycle.

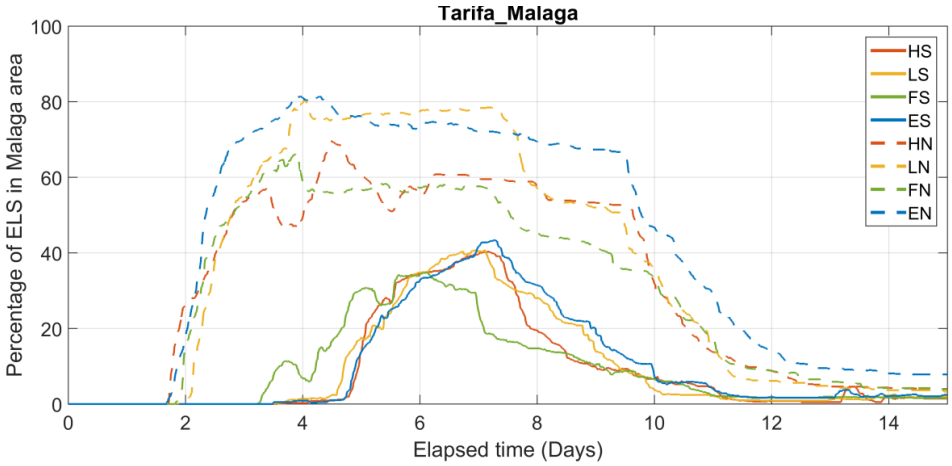

Figure 13. Percentages of ELS released at surface in Tarifa and found in Malaga box over the elapsed time under different tidal conditions. Line style coding is the same used in Figure 12.

In order to determine the spatial variability according to the different depth levels, the corresponding connectivity percentages were computed for the Estepona box, as an explicit example (Figure 14).

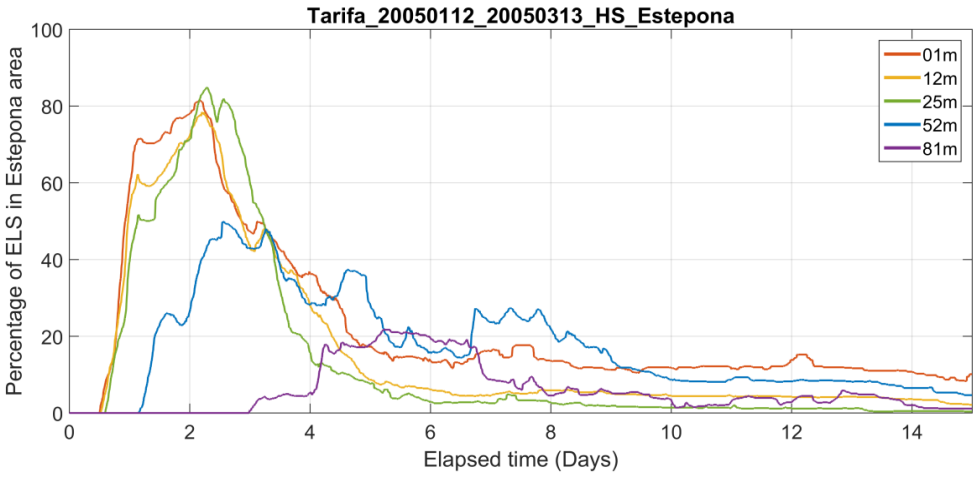

Figure 14. Percentages of ELS released in Tarifa and found in Estepona box over the elapsed time under the HS condition for the 5 depth levels.

As expected, the highest percentages are found in the surface layers, as a consequence of the AJ dominance. Whilst the most surface layers (1m, 12m and 25m) reach a maximum of ≈80% ELS, the 52m and 81m levels shows a maximum value of ≈40% ELS and ≈20% ELS respectively.

Due to the main predominance of the zonal transport over the meridional, the opposite situation is reflected at the southern boundary of the Alboran Sea. In this region, percentages registered in the connectivity boxes are generally lower compared to the opposite margin. Within these boxes, Oran is one of the most similar boxes compared with the northern case. Further than sporting the highest percentages of the southern margin (13.69% ± 0.48%), this box has also a similar dynamics to Estepona box, possibly due to the AJ that follows the Almería-Oran front and flow toward the Argelian coast.

Nevertheless, although the deepest level (81 m) continues to be the least connected layer, the surface layer predominance is not as evident as the previous case, perhaps because this area does not receive a direct influence of the AJ. This means, there is a greater variability between the different release depths, with a slightly higher influence of the 25 m depth level (with a difference of ≈15% ELS with the surface layer).

Finally, as previously mentioned, the surface connectivity between the boxes from the Alboran Sea toward the Atlantic Ocean is highly improbable due to the high influence of the jet inflow. Nevertheless, a small percentage of particles can be exceptionally leaped as a consequence of a possible tidal slowdown. For this area, a mean of 1% ELS were registered in the Cadiz box under the Low Tide-Spring Cycle, and not a single particle was found in the Arcila box.

The second map (Figure 10) shows values of ELS (%) released from Tanger and predominantly advected along the southern margin of the Alboran Sea, being higher at Tetuan (32.60% ± 0.42%) and Alucemas (13.75% ± 1.04%) boxes.

Tetuan box, which is the closest to the starting area in this case, is the one that has the highest percentages because of the high influence of the tidal dynamics, with preponderance of the ELS percentages under the spring tide (Figure 15).

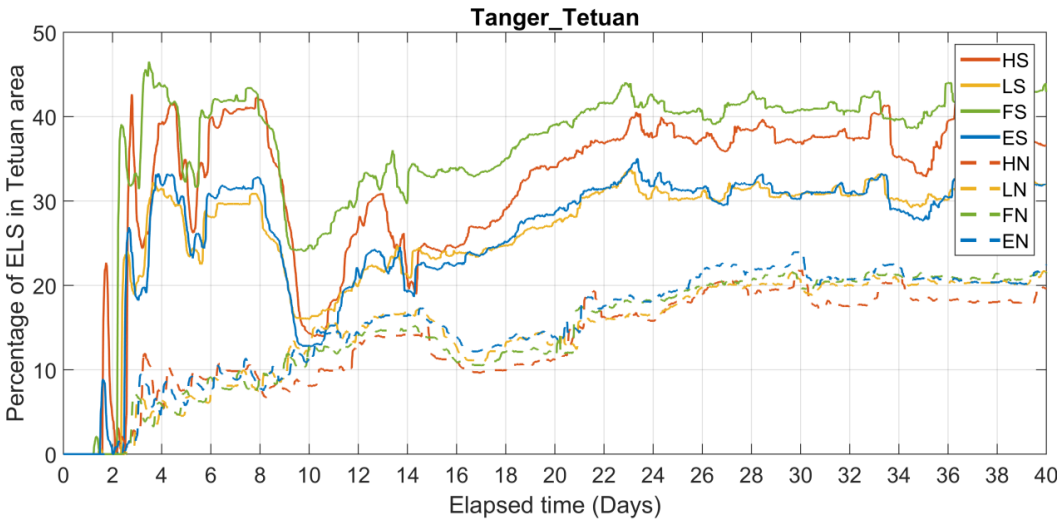

Figure 15. Percentages of ELS released at surface in Tarifa and found in Malaga box over the elapsed time under different tidal conditions.

In this specific analysis the ELS percentages under all the tidal phase combinations with the neap cycle are maintained at relatively stable values, and the velocity is remarkably uniform along the complete elapsed time, whilst during the spring cycle, the ELS percentages are more susceptible to variation, possibly due to higher velocity of the particles under this condition. Moreover, from the 14 day forward, a stability of the ELS percentages in both combinations of tides is observed, probably due to a self-recruitment of the propagules under those circumstances.

Figure 15 is also a clear example of why a fixed time metric would not have been convenient for this particular study. Due to the high tidal dynamics influence registered in Tetuan box, a consequent high variability is represented during the first 4 days of the simulation. The first day, the percentages of ELS under HS, LS, FS and ES ascend quickly to 20% but, immediately to this rise, they drop rapidly to 0%. After the second day approximately, the percentages ascends again sharply reaching a maximum of 45% and, then, they go back down again to 20%, staying in this oscillation dynamics until day 12. This means, if for example only the second and third days would have been taken into account for this particular analysis, 0% and 20% ELS would have been registered respectively (instead of 20% and 45%), causing an underestimation of the results and, therefore, a no-representative calculation of the real situation.

Alucemas box does not reflect the same dynamics variability as Tetuan box, but it is a clear example of a slower dynamic that involves the whole domain of the WAG gyre; this means, despite of its proximity to the SoG, the results of the ELS percentages are insignificant compared to the left adjoining box, probably due to the particles, once crossing the Tetuan box, are transported within the WAG gyre and is not until they go through the whole gyre when the particles reach this box, with a preponderance of 25 m, as can be observed in Figure 16. For this reason, the times at which these percentages are reached are very high (between 40 and 60 days, approximately. Despite of all the depth levels show coherent behaviors according to this suggestion, the 25 m level leaps this average tendency, likely due to the main pathway of theses trajectories that touch the northern boundary of the box and determine notable difference with small deviations in latitude.

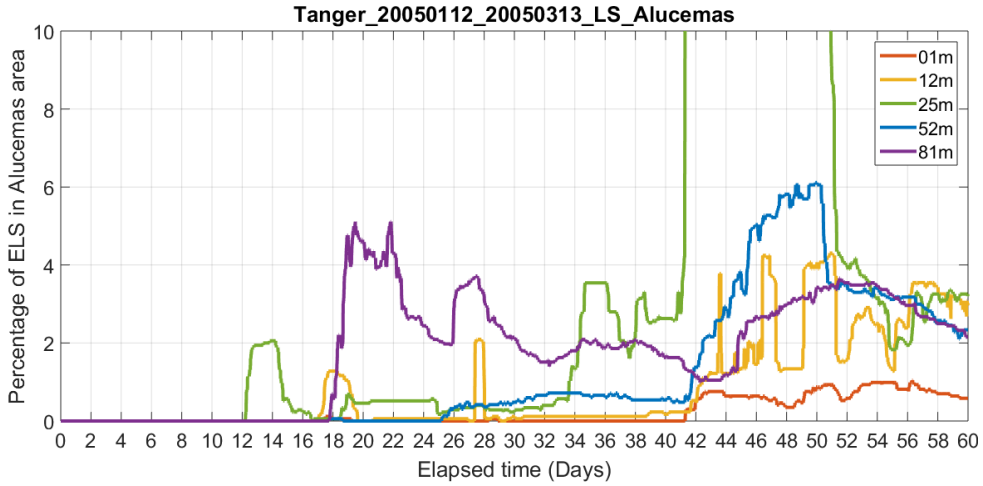

Figure 16. Percentages of ELS released in Tanger and found in Alucemas box over the elapsed time under the LS condition for the 5 depth levels.

As the previous area, the ELS percentages registered at the northern boundary are higher under neap cycles, being most evident in Roquetas and Melilla boxes, affirming a high dispersion of the particles under this tidal cycle. Finally, a low percentage of ELS were registered for this particular case in the Arcila box, reaching a maximum of 8% under Low Tide-Spring Cycle (the same tide combinations of the particles registered in Cadiz in the previous case), affirming a slowdown in this specific tide combination.

The third map (Figure 11) shows values of ELS (%) released from TangerMED highly similar to Tanger, and predominantly advected along the southern margin of the Alboran Sea, being higher at Tetuan (44.91% ± 0.48%) and Alucemas (17.33% ± 0.97%) boxes.

As the previous case, Tetuan is the most dynamic box because of the high dynamics influence. However, in this case ELS percentages registered in this box are higher than the released from Tanger, probably due to its major proximity to the connectivity box. Alucemas has a preponderance of the 25 m too. Moreover, the boxes of the northern boundary have a preponderance of the percentages at deep layers. Finally, instead of the Tanger case, the ELS percentages registered at the Atlantic boxes are minimum, probably because of its proximity to the Alboran Sea as well as the smaller size of this polygon.

The clear similarities between Tanger and TangerMED boxes (Figure 17), as well as it high differences with Tarifa, confirm the fact that the main transport is zonal instead of meridional, and that the AJ acts as a barrier for the connectivity patterns. Furthermore, it is known that the central part of the SoG, where the Tanger box is located, is more dynamically biased to the south and more isolated from the north with respect to the south mainly due geostrophic balance (Albérolaa *et al.*, 1995).

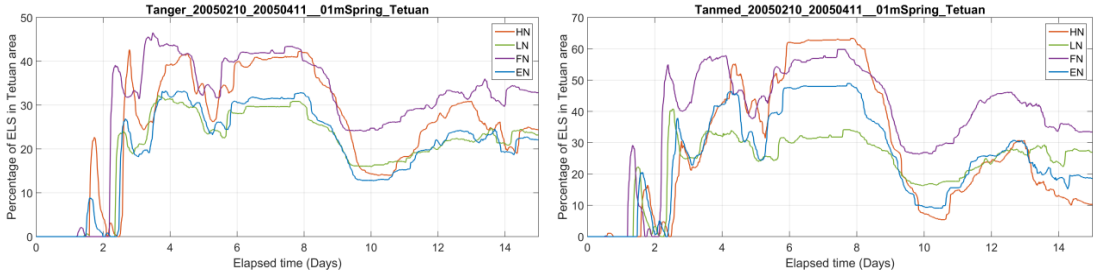

Figure 17. Differences between the ELS percentages registered at surface under spring cycle in Tetuan from Tanger(left) and TangerMED(right).

In order to analyse the differences between the LPT, all the individual trajectories of the passive particles advected by the currents from the three release areas were plotted (Figure 18 for Tarifa case, Figure 19 for Tanger case and Figure 20 for TangerMED case). In these maps, each individual line represents the trajectory of an individual particle. Within the three cases, Tarifa was the release areas that shows a most marked pattern of both the Alboran gyres (WAG+EAG). Despite of Tanger and TangerMED areas show a clear influence of the WAG, they did not show a clearly pattern through the EAG. Thus, it could be said that the most adapted box to the general circulations patterns of the Alboran Sea is Tarifa.

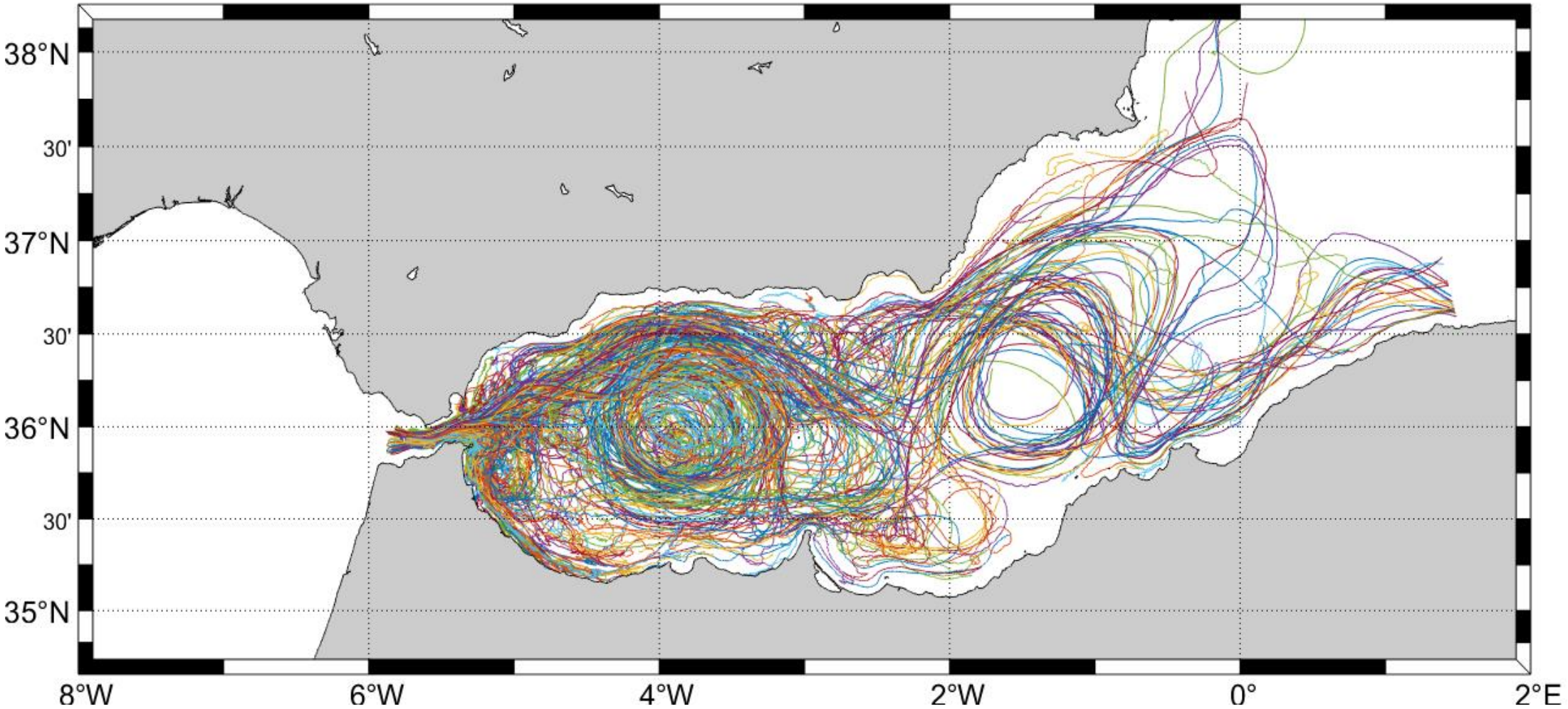

Figure 18. Trajectories of the particles released from Tarifa.

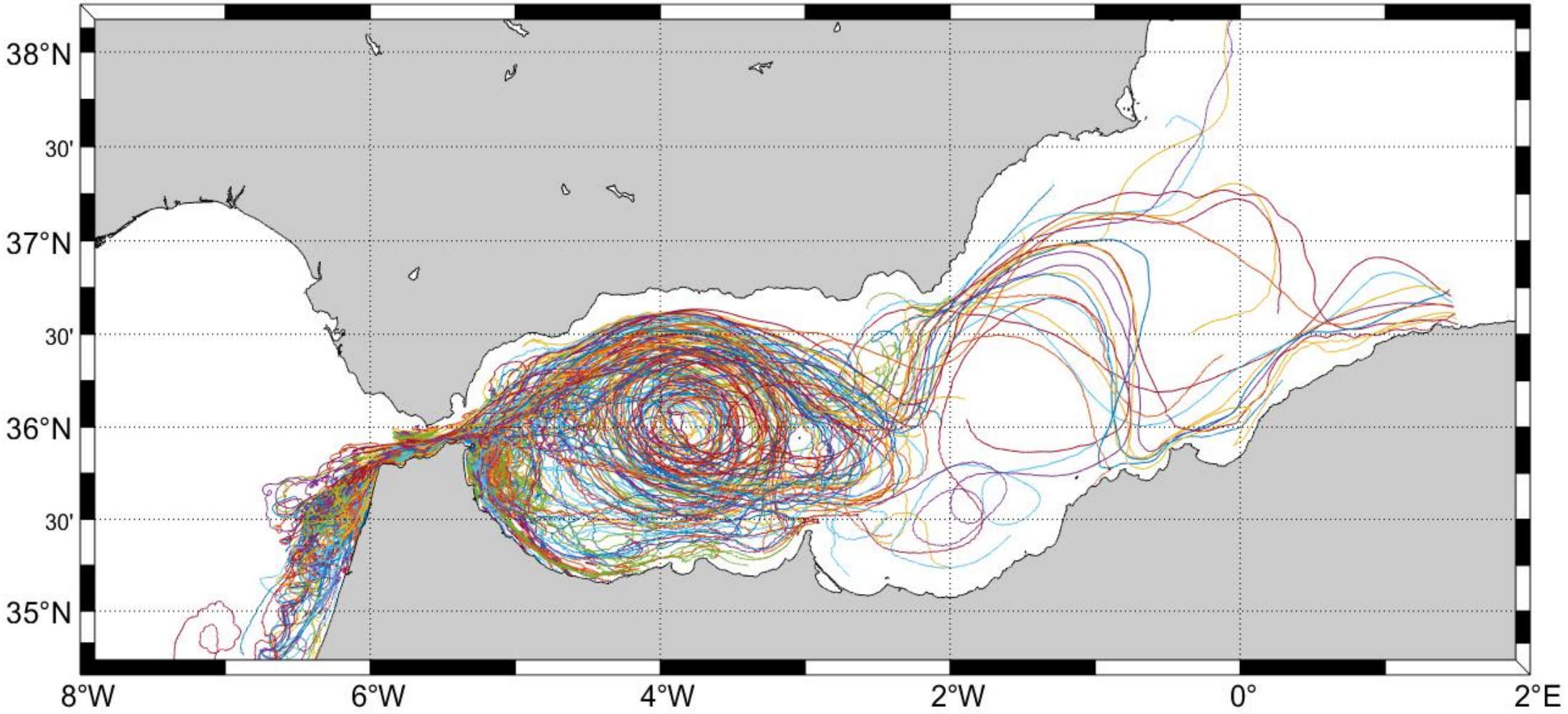

Figure 19. Trajectories of the particles released from Tanger.

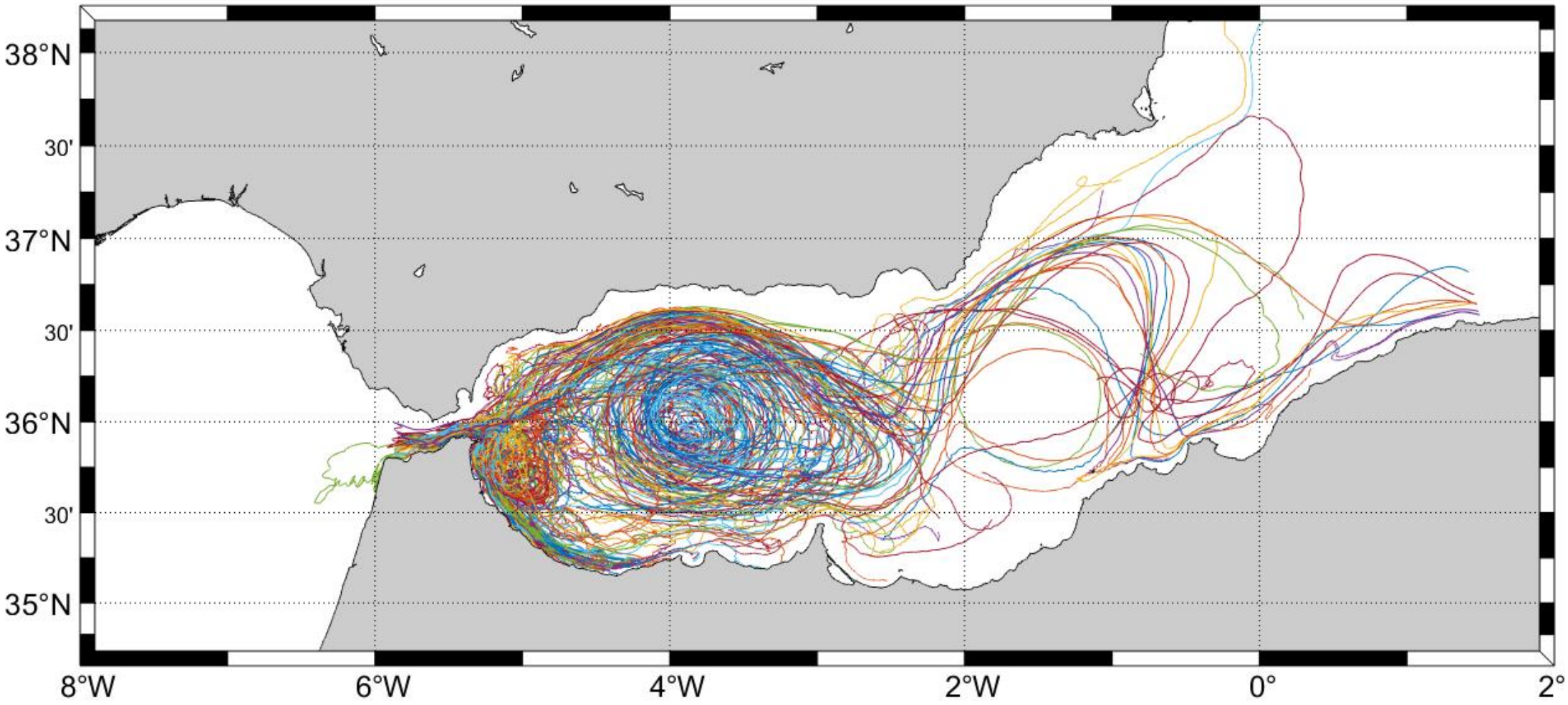

Figure 20. Trajectories of the particles released from TangerMED.

After the simulations of the forth repeated simulations of the same tidal conditions, it could be observed that the internal variability (intra-class) between them was relatively homogenous and lower than the estimated external variability (inter-class), i.e., the simulations of different tidal conditions. Even so, due to the different forcings applied to the model are based in real data and not on climatologies, is expected that the intra-class simulations, still being very similar but not null, vary slightly. If this is true, it could be said that the replicas are enough robust and the box is enough small to affirm that the four simulations can characterize the dynamics of a whole specific box. Figure 21 shows an example of the difference between two replicas (the first and the third) of a same tidal condition.

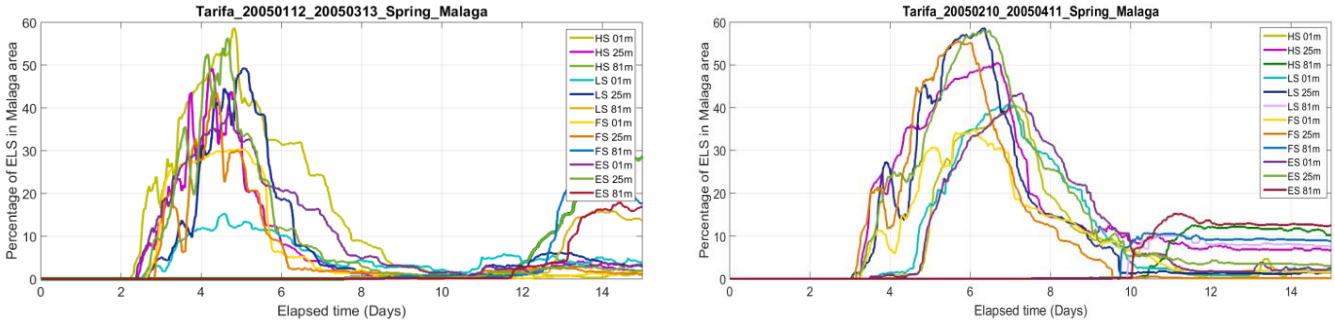

Figure 21. Differences of percentages of ELS registered between the first and the third replica of Tarifa under spring conditions.

Moreover, in any statistical approach it is estimated that, in order to ensure the representativeness as well as the reliability of the model results, at least 3 replicas of the whole same experiment have to be done (ASTM E122-17, 2017). With the aim of determining the differences, an example of replica was done for the Ebb Neap tide and there were hardly any differences between the results. Figure 22 shows the difference of the sea level in cm between one EN and the following. Figure 23 shows the difference in percentage of ELS over the time.

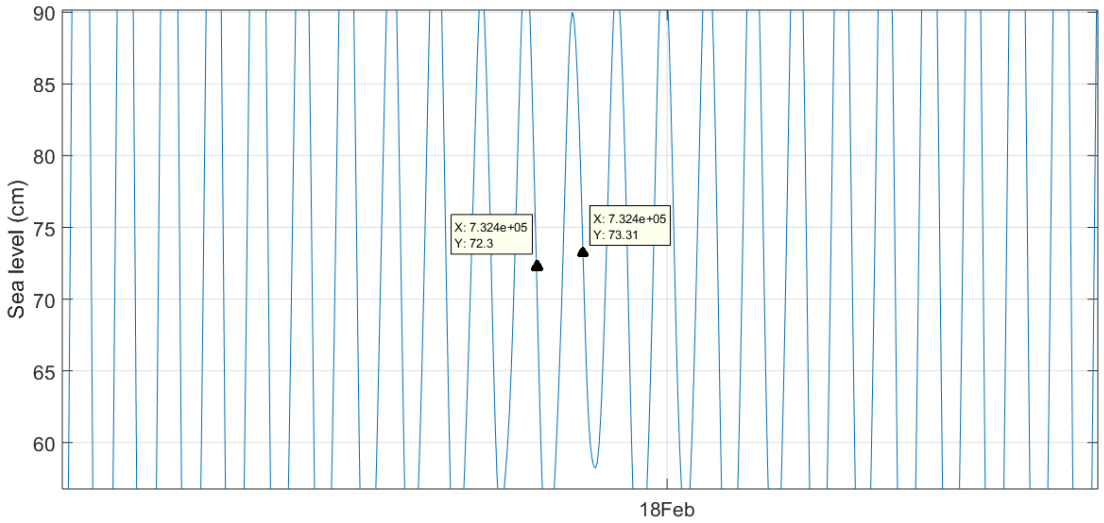

Figure 22. Differences in sea level (cm) between two replicas of EN.

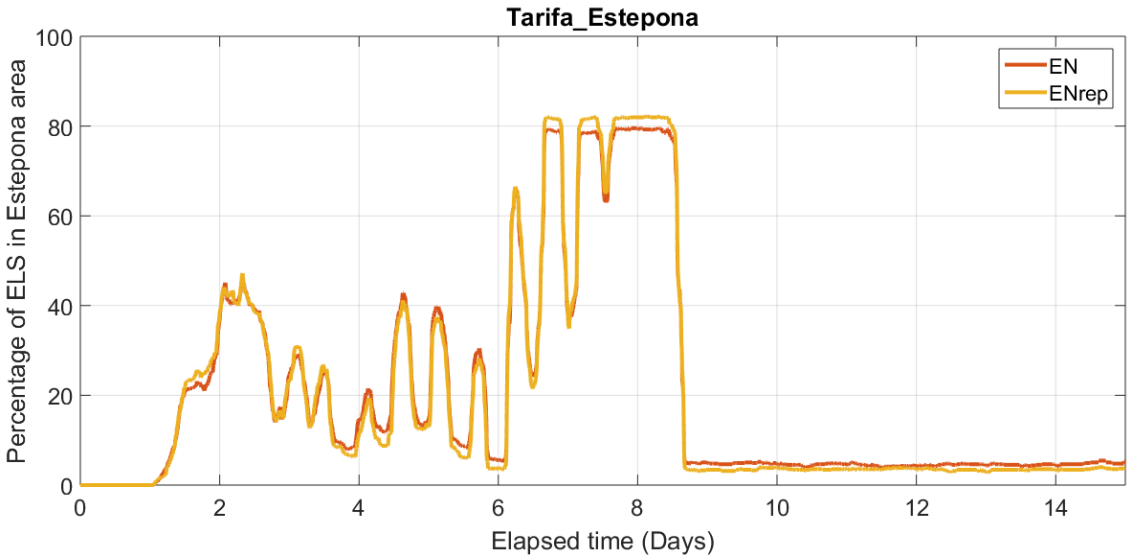

Figure 23. Differences in the ELS percentages over the time between the two replicas of EN00.

VII. Conclusions

After the numerical experiment, it could be confirmed that the hydrodynamic model adapted to a lagrangian approach is the most appropriated tool for the study of connectivity, dispersal patterns and population dynamics of the blackspot seabream in the SoG under the effect of tidal dynamics, and is necessary towards a better management of the *voracera's* fleets.

However, to prove the representativeness and reliability of the model, several sensitivity analyses according to the spatial and the temporal variability are needed. In this particular case, a total of five depths between the surface and 81m and three release areas located within the SoG (further than the ten release boxes distributed by

the Alboran sea and the eastern limit of the SoG) were defined in order to determine the spatial variability of the model results. Moreover, eight tide conditions (according to the tidal phase and strength) were defined in order to determine the effects of the tides in the connectivity and dispersal patterns. Finally, four replicas were defined in order to prove different results under the same tidal and spatial conditions but with different time series. Thus, the experiments sum 160 runs per release area, with a total of 480 runs. Thus, the computational cost that an experiment of this ambit requires is considerably high and only advanced supercomputing resources can solve them.

As it is considered that once the blackspot seabreams overcome the ELS, they develop enough swimming capacity for not being transported passively by the tides, eggs and larvae were used to the simulations. Furthermore, due to the Pelagic Larval Duration of this species lasts between 40 and 60 days, each simulation was 60 days long.

After the interpretation of the results obtained, the most remarkable dynamic that can be concluded is that fortnightly modulation (spring tide-neap tide) has a greater effect on the connectivity patterns and horizontal dispersion than the tidal phase. Within the tide modulation, the neap tides generally resulted in a lower dispersion and more uniform velocities, while spring tides resulted in higher velocities and higher dispersion. Particles released in Tarifa were registered predominantly in the northern boundary of the Alboran sea, whilst particles released in Tanger and TangerMED were registered in the southern boundary. Instead, few particles were registered at the Atlantic Ocean, demonstrating the AJ predominance Finally, the variability according to the depth level shown a higher energy and, thus, higher percentages on the most superficial levels.

VIII. References

Albérolaa, C., Rousseau, S. and Millot, C. (1995) 'Tidal currents in the western Mediterranean Sea', vol. 18, pp. 273–284.

Álvarez Fanjul, E., Pérez Gómez, B. and Sánchez-Arévalo, I. R. (2001) 'Nivmar : A storm surge forecasting system for Spanish Waters', vol. 65, pp. 145–154.

ASTM E122-17 (2017) 'Standard Practice for Calculating Sample Size to Estimate, With Specified Precision, the Average for a Characteristic of a Lot or Process', *ASTM International,* [Online]. DOI: 10.1520/E0122-17.

Botsford, L. W., Brumbaugh, Æ. D. R., Grimes, Æ. C., Kellner, J. B., Largier, Æ. J., Farrell, Æ. M. R. O., Ralston, Æ. S., Soulanille, E. and Wespestad, Æ. V. (2009) 'Connectivity , sustainability , and yield : bridging the gap between conventional fisheries management and marine protected areas', pp. 69–95 [Online]. DOI: 10.1007/s11160-008-9092-z.

Candela, J., Winant, C. and Ruiz-Cañavate, A. (1990) 'Tides in the Strait of Gibraltar', *Journal of Geophysical Research Atmospheres*, vol. 95(C5):731 [Online]. DOI: 10.1029/JC095iC05p07313.

Cowen, R. K. and Sponaugle, S. (2009) 'Larval Dispersal and Marine Population Connectivity', [Online]. DOI: 10.1146/annurev.marine.010908.163757.

Feist, B. E., Torgersen, C. E., Miller, D. J., Sanderson, B. L., Northwest, P., Ecosystem, R. and Station, C. F. (2010) 'Hydrological connectivity for riverine fish : measurement challenges and research opportunities', [Online]. DOI: 10.1111/j.1365-2427.2010.02448.x.

Fuller, E. C., Samhouri, J. F., Stoll, J. S., Levin, S. A. and Watson, J. R. (2017) 'Editor ' s Choice Characterizing fisheries connectivity in marine social – ecological systems', vol. 74, pp. 2087–2096 [Online]. DOI: 10.1093/icesjms/fsx128.

García Lafuente, J., Álvarez Fanjul, E., Vargas, J. M. and Ratsimandresy, A. W. (2002) 'Subinertial variability in the flow through the Strait of Gibraltar', *Journal of Geophysical Research: Oceans*, vol. 107, no. C10, p. 3168 [Online]. DOI: http://dx.doi.org/10.1029/2001JC001104.

García Lafuente, J., Bruque Pozas, E., Sánchez Garrido, J. C., Sannino, G. and Sammartino, S. (2013) 'The interface mixing layer and the tidal dynamics at the eastern part of the Strait of Gibraltar', *Journal of Marine Systems*, vol. 117–118, no. 0, pp. 31–42 [Online]. DOI: http://dx.doi.org/10.1016/j.jmarsys.2013.02.014.

García Lafuente, J., Vargas, J. M., Plaza, F., Sarhan, T., Candela, J., Bascheck, B., García-Lafuente, J., Vargas, J. M., Plaza, F., Sarhan, T., Candela, J. and Bascheck, B. (2000) 'Tide at the eastern section of the Strait of Gibraltar', *Journal of Geophysical Research: Oceans*, vol. 105, no. C6, pp. 14197–14213 [Online]. DOI: http://dx.doi.org/10.1029/2000JC900007.

García, T., Báez, J., Baro, J., García, A. and Giráldez, A. (2012) 'Fishery in Alborán Sea', no. June [Online]. DOI: 10.13140/RG.2.1.3412.0160.

Gil Herrera, J. (2006) 'Biologia y pesca del voraz [Pagellus bogaraveo (Brünnich , 1768)]',.

ICES (2018) *Blackspot sea bream (Pagellus bogaraveo) in Subarea 9 (Atlantic Iberian waters)*, [Online]. DOI: 10.17895/ices.pub.4402.

LaCasce, J. H. (2008) ‘Statistics from Lagrangian observations’, *Progress in Oceanography*, vol. 77, no. 1, pp. 1–29 [Online]. DOI: 10.1016/j.pocean.2008.02.002.

Lafuente, J. G., Cano, N., Vargas, M., Rubín, J. P. and Hernández-Guerra, A. (1998) ‘Evolution of the Alboran Sea hydrographic structures during July 1993’, *Deep-Sea Research Part I: Oceanographic Research Papers*, vol. 45, no. 1, pp. 39–65 [Online]. DOI: 10.1016/S0967-0637(97)00216-1.

Lafuente, J. G., Delgado, J., Vargas, J. M., Vargas, M., Plaza, F. and Sarhan, T. (2002) ‘Low-frequency variability of the exchanged flows through the Strait of Gibraltar during CANIGO’, *Deep-Sea Research Part II: Topical Studies in Oceanography*, vol. 49, no. 19, pp. 4051–4067 [Online]. DOI: 10.1016/S0967-0645(02)00142-X.

Marshall, J., Adcroft, A., Hill, C., Perelman, L. and Heisey, C. (1997) ‘A finite-volume, incompressible navier stokes model for, studies of the ocean on parallel computers’, *Journal of Geophysical Research C: Oceans*, vol. 102, no. C3, pp. 5753–5766 [Online]. DOI: 10.1029/96JC02775.

Muñoz, M., Reul, A., Plaza, F., Gomez-Moreno, M., Vargas-Yáñez, M., Rodríguez, V. and Rodríguez, J. (2015) ‘Ocean & Coastal Management Implication of regionalization and connectivity analysis for marine spatial planning and coastal management in the Gulf of Cadiz and Alboran Sea’, pp. 1–15 [Online]. DOI: 10.1016/j.ocecoaman.2015.04.011.

Navarro, G., Vzquez, Á., MacÍas, D., Bruno, M. and Ruiz, J. (2011) ‘Understanding the patterns of biological response to physical forcing in the Alborn Sea (western Mediterranean)’, *Geophysical Research Letters*, vol. 38, no. 23, pp. 1–5 [Online]. DOI: 10.1029/2011GL049708.

Renault, L., Oguz, T., Pascual, A., Vizoso, G. and Tintore, J. (2012) ‘Surface circulation in the Alborn Sea (western Mediterranean) inferred from remotely sensed data’, *Journal of Geophysical Research: Oceans*, vol. 117, no. 8, pp. 1–11 [Online]. DOI: 10.1029/2011JC007659.

Reul, A., Rodríguez, V., Jiménez-Gómez, F., Blanco, J. M., Bautista, B., Sarhan, T., Guerrero, F., Ruíz, J. and García-Lafuente, J. (2005) ‘Variability in the spatio-temporal distribution and size-structure of phytoplankton across an upwelling area in the NW-Alboran Sea, (W-Mediterranean)’, *Continental Shelf Research*, vol. 25, no. 5–6, pp. 589–608 [Online]. DOI: 10.1016/j.csr.2004.09.016.

Rodríguez, J. (1982) *Oceanografía del Mar Mediterráneo*, Piramide (ed).

Sahyoun, R., Guidetti, P., Franco, A., Planes, S., Sahyoun, R., Guidetti, P., Franco, A., Planes, S., Connectivity, F., Sahyoun, R., Guidetti, P., Franco, A. Di and Planes, S. (2017) ‘Patterns of Fish Connectivity between a Marine Protected Area and Surrounding Fished Areas To cite this version : HAL Id : hal-01442055 Patterns of Fish Connectivity between a Marine Protected Area and Surrounding Fished Areas’, [Online]. DOI: 10.1371/journal.pone.0167441.

Sammartino, S., García Lafuente, J., Sánchez Garrido, J. C., De los Santos, F. J., Álvarez Fanjul, E., Naranjo, C., Bruno, M. and Calero, C. (2014) ‘A numerical model analysis of the tidal flows in the Bay of Algeciras, Strait of Gibraltar’, *Continental Shelf Research*, vol. 72, pp. 34–46 [Online]. DOI: 10.1016/j.csr.2013.11.002.

Sammartino, S., Sánchez Garrido, J. C., García Lafuente, J., Naranjo, C., Hidalgo, M. and Gil Herrera, J. (2018) ‘Modelling the dispersion of early life stages of blackspot seabream in the Strait of Gibraltar’, *FISHFORUM*, p. 1300216.

Sánchez Garrido, J. C., García Lafuente, J., Álvarez Fanjul, E., Sotillo, M. G. and de los Santos, F. J. (2013) 'What does cause the collapse of the Western Alboran Gyre? Results of an operational ocean model', *Progress in Oceanography*, vol. 116, no. 0, pp. 142–153 [Online]. DOI: http://dx.doi.org/10.1016/j.pocean.2013.07.002.

Sánchez Garrido, J. C., Naranjo, C., Macías, D., García-Lafuente, J. and Oguz, T. (2015) 'Modeling the impact of tidal flows on the biological productivity of the Alboran Sea', *Journal of Geophysical Research: Oceans*, vol. 120, no. 11, pp. 7329–7345 [Online]. DOI: 10.1002/2015JC010885.

Sarhan, T., García Lafuente, J., Vargas, M., Vargas, J. M., Plaza, F., Garcı́a Lafuente, J., Vargas, M., Vargas, J. M. and Plaza, F. (2000) 'Upwelling mechanisms in the northwestern Alboran Sea', *Journal of Marine Systems*, Elsevier, vol. 23, no. 4, pp. 317–331 [Online]. DOI: http://dx.doi.org/10.1016/S0924-7963(99)00068-8.

Sotillo, M. G., Cailleau, S., Lorente, P., Levier, B., Aznar, R., Reffray, G., Amo-Baladrón, A., Chanut, J., Benkiran, M. and Alvarez-Fanjul, E. (2015) 'The MyOcean IBI Ocean Forecast and Reanalysis Systems: operational products and roadmap to the future Copernicus Service', *Journal of Operational Oceanography*, Taylor & Francis, vol. 8, no. 1, pp. 63–79 [Online]. DOI: 10.1080/1755876X.2015.1014663.

Toucanne, S., Jouet, G., Ducassou, E., Bassetti, M., Dennielou, B., Morelle, C., Minto, A., Lahmi, M., Touyet, N., Charlier, K. and Lericolais, G. (2014) 'A 130 , 000-year record of Levantine Intermediate Water flow variability in the Corsica Trough , western Mediterranean Sea', pp. 95–96.

UNEP (2014) 'Status of the open sea fisheries in the Alboran Sea', no. April, pp. 7–11.

Urban, D. L. and Pratson, Æ. L. F. (2008) 'Modeling population connectivity by ocean currents , a graph-theoretic approach for marine conservation Modeling population connectivity by ocean currents , a graph-theoretic approach for marine conservation', no. February 2014 [Online]. DOI: 10.1007/s10980-007-9138-y.

Vargas-Yáñez, M., Plaza, F., García-Lafuente, J., Sarhan, T., Vargas, J. . M. and Vélez-Belchi, P. (2002) 'About the seasonal variability of the Alboran Sea circulation', *Journal of Marine Systems*, vol. 35, pp. 229–248.